Electronic Supplementary Material (ESI) for Journal of Materials Chemistry A.
This journal is © The Royal Society of Chemistry 20xx

Supporting Information

A Hierarchical Heterojunction Polymer Aerogel for Accelerating Charge Transfer and Separation

Yue Yin, Chongbei Wu, Guanhang Yu, Haozhen Wang, Qing Han, and Liangti Qu*

Y. Yin, C. Wu, G. Yu, H. Wang, Dr. Q. Han
Key Laboratory of Photoelectronic/Electrophotonic Conversion Materials
Key Laboratory of Cluster Science
Ministry of Education of China
School of Chemistry and Chemical Engineering
Beijing Institute of Technology
Beijing 100081, P. R. China.
E-mail: qhan@bit.edu.cn

Prof. L. Qu
Department of Chemistry
Tsinghua University
Beijing 100084, China.

Experimental Section

Chemicals: All reagents were used without further purification. Dicyandiamide (DCDA) and Formic acid (HCOOH, 88%) were purchased from Aladdin.

Synthesis of g-C_3N_4

2 g DCDA was put into an alumina crucible with a cover, then calcined at 500 ºC for 4 h in N_2 with heating rate of 2 °C/min. After cooling to room temperature naturally, the collected sample was ground to homogeneous powder and denoted as g-C_3N_4.

Synthesis of HPP

HPP was synthesized by the previous report with a slight modification.[1] Typically, a 0.5 g/mL mixture solution of formic acid/DCDA with stoichiometry ratio of 0.4 was kept at 130 °C for 6 h, and then dried overnight. Last, the obtained sample was ground into powders, followed by heating at 550 ºC with a ramp rate of 5 °C/min in N_2 and kept for 4 h.

Synthesis of HPA

A certain amount of DCDA were added to 60 mL deionized water, then stirred for 30 min to obtain a homogeneous solution. The solution was transferred into a Teflon-lined autoclave at 200 ºC for 4 h. After cooling to room temperature, hydrothermally treated dicyandiamide (HTD) was refluxed with a certain amount of formic acid at 100 ºC for 2 h, and then kept in liquid nitrogen to freeze dry. Finally, the resultant white power was heated to 500 ºC in a tubular furnace with a ramp rate of 2 ºC/min in N_2 and kept for 4 h. The obtained sample was denoted as HPA_x (x=0.1, 0.2, 0.3, 0.5, x represents the stoichiometric ratio of formic acid/HTD).

Characterization

Scanning electron microscopy (SEM, JSM-7500) and transmission electron microscopy (TEM, 7650B, Hitachi) were utilized to obtain the morphology and composition of samples.

Power X-ray diffraction (PXRD) was carried out by a 1710 diffractometer with a Cu K*a* irradiation source (λ=1.5418 Å). The function groups of samples were determined by Fourier transform infrared (FTIR, Equinox 55/S) between 500-4000 cm^{-1}. Raman spectroscopy was conducted by LabRAM HR Evolution from Horiba. Solid state ^{13}C NMR spectra was reported on a JNM-ECZ600R spectrometer. The chemical status was performed by X-ray photoelectron spectroscopy (XPS) measurements using an ESCALab220i-XL electron spectrometer from VG Scientific. Optical diffuse reflectance spectra were measured with a Shimadzu UV-3600 UV-vis-NIR spectrometer. Photoluminescence (PL) spectroscopy was undertaken using a fluorescence spectrophotometer (Edinburgh, FLSP920) upon excitation at 340 nm. Electron paramagnetic response (EPR) spectra was obtained using a JES-FA200 ESR Spectrometer at room temperature.

Photocatalytic activity tests

Photocatalytic hydrogen production experiments were achieved in a top-irradiation reactor attached to a gas-closed glass system. 10 mg photocatalyst was dispersed in a mixed solution containing 90 mL deionized water and 10 mL methanol as the sacrificial electron donor. 3 wt% Pt (using H_2PtCl_6 as a precursor) was in situ photo-deposited on the photocatalysts as the cocatalyst. Prior to irradiation under a 300 W Xenon arc lamp (CEL-HXF300, Au-Light, China) equipped with a 380 nm cutoff filter, the reactor was sealed and degassed under vacuum to thoroughly remove air. The temperature of the solution was stabilized at 6 ºC throughout the reaction by a flow of cooling water. The generated H_2 was analyzed by gas chromatograph (GC-2014C Shimadzu) with high-purity argon carrier gas. The internal quantum yield (IQY) of photocatalyst was measured under 300 W Xe lamp (equipped with band pass filter of 400 nm) irradiation. The active area of the reactor was approximately 12.56 cm^2. The monochromatic light (400 nm) intensity was averaged at 5 representative points with PL-MW2000 Photoradiometer. 50 mg catalyst was dispersed into 80 mL aqueous solution containing 10

vol.% methanol and 3 wt% H_2PtCl_6 (with respect to the catalyst used). Therefore the average light intensity at 400 nm was calculated to be 35.8 mW. Then, IQY was calculated as follows:

$$IQY = \frac{2 \times amount\ of\ hydrogen\ molecules\ evoled}{number\ of\ absorbed\ photons} \times 100\% \quad (1)$$

$$Number\ of\ absorbed\ photons\ (N_{absored\ photons}) = N_1 - N_2 \ (2)$$

in which, N_1 represented the number of incident photons that was measured without photocatalysts, N_2 represented the number of incident photons that was measured after adding the photocatalysts. The number of absorbed photons for the IQY was the difference between N_1 and N_2.

The external quantum yield (EQY) of photocatalyst was measured under 300 W Xe lamp (equipped with band pass filter of 400 nm) irradiation. The active area of the reactor was approximately 12.56 cm^2. The monochromatic light intensity was averaged at 5 representative points with PL-MW2000 Photoradiometer. Therefore the average light intensity at 400 nm was calculated to be 68.7 mW. Then, the $HPA_{0.2}$ in our work shows the EQY of 15.3% at 400 nm. The EQY was calculated by the following Equation (3):

$$EQY = \frac{2 \times amount\ of\ hydrogen\ molecules\ evoled}{number\ of\ incident\ photons} \times 100\% \quad (3)$$

Electrochemical measurements

Electrochemical measurements were monitored in 0.2 M Na_2SO_4 electrolyte solution on a CHI 760E electrochemical work station equipped a standard three-electrode system, in which samples-coated FTO glass, Pt sheet and Ag/AgCl (saturated KCl) electrode were acted as the working electrode, counter electrode and reference electrode, respectively. Specifically, the preparation of the working electrode was as follows: 5 mg photocatalyst was suspended in a mixed solution containing 10 μL of Nafion solution (5 wt%) and 1 mL ethanol, then ultrasonic

treated about 60 min to obtain a homogeneous slurry. Then the resultant slurry was coated on FTO glass with area of ~1 cm^2 and then dried in a 50 ℃ oven.

EPR normalization calculation

By integrating the first differential curve for twice, the area of the absorption curve was calculated and compared with a standard sample containing a known number of single electrons to measure the single electron content in the sample.[3] Mn marker signal was used to calibrate the signal intensity of the samples. As is shown in the following formula, the relative change in the number of spins ($N_x/N_{HPA0.2}$) could be calculated.

$$\frac{Nx}{N_{HPA0.2}} = \frac{I_x}{I_{HPA0.2}} * \frac{J_{Mn,HPA0.2}}{J_{Mn,x}} * \frac{m_{HPA0.2}}{m_x}$$

Where N_x represented the number of spins contained in the sample, and $N_{HPA0.2}$ represented the number of spins in the $HPA_{0.2}$ sample. $I_x/I_{HPA0.2}$ represented the second integral value of a certain signal in the sample, $J_x/J_{Mn,\ HPA0.2}$ represented the double integral value of a certain signal in the sample, based on Mn as the marker signal. $m_{HNPA0.2}/m_x$ represented the quality of the measured sample.[3]

Results and Discussion

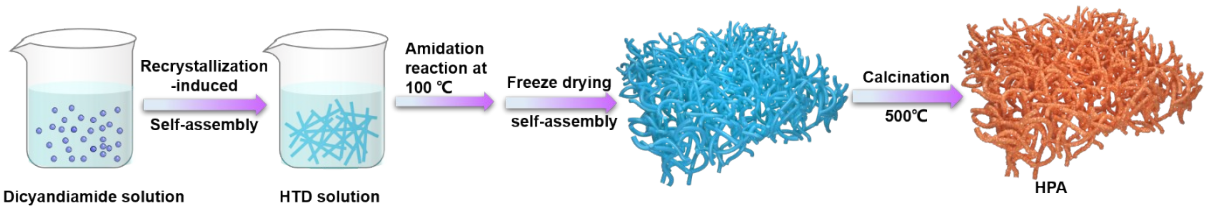

Figure S1. Experimental procedure for fabrication of HPA.

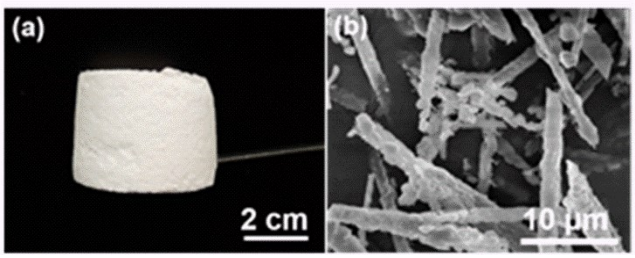

Figure S2. a) Photograph, b) SEM image of the frozen fibrous mixture precursor.

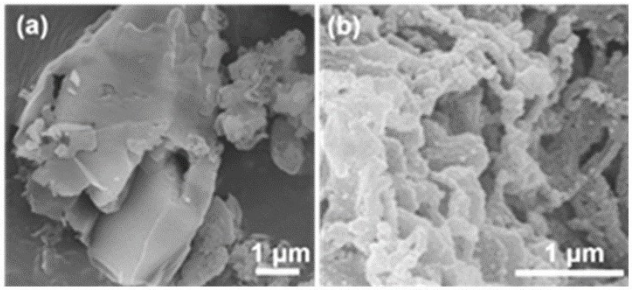

Figure S3. SEM images of a) g-C_3N_4. b) HPP.

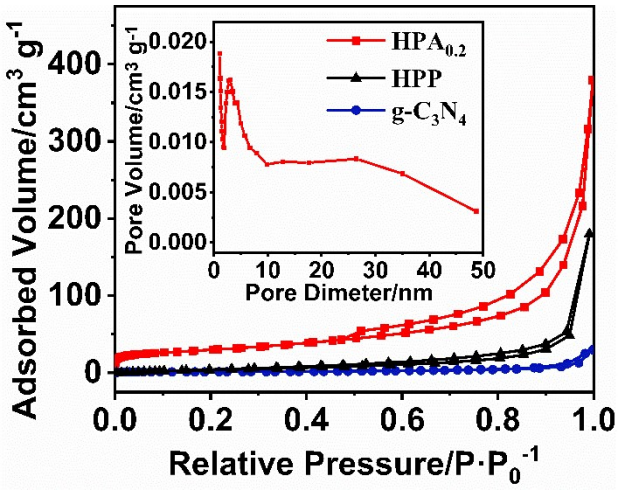

Figure S4. N_2 adsorption isotherms of g-C_3N_4, HPP and $HPA_{0.2}$. The inset is the pore size distribution of $HPA_{0.2}$.

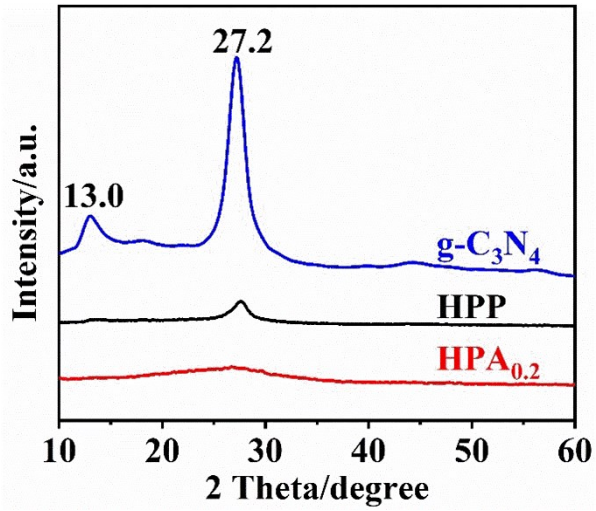

Figure S5. XRD patterns of g-C_3N_4, HPP and $HPA_{0.2}$.

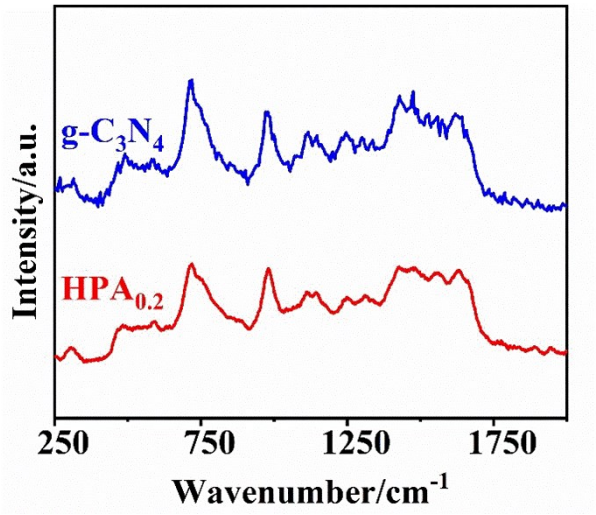

Figure S6. Raman spectra of g-C_3N_4 and $HPA_{0.2}$.

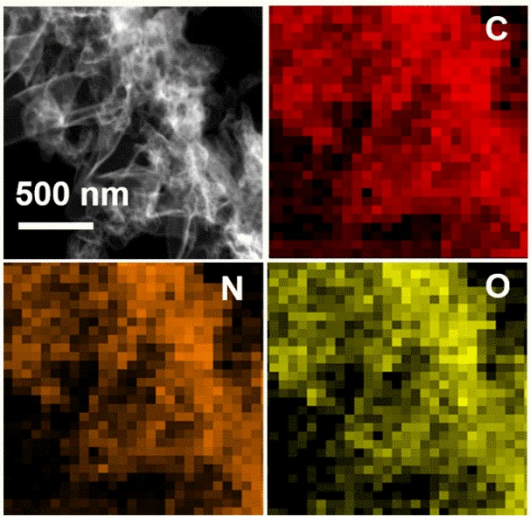

Figure S7. HAADF-STEM image and the corresponding HAADFSTEM-EDS C, N, O element mapping images of $HPA_{0.2}$.

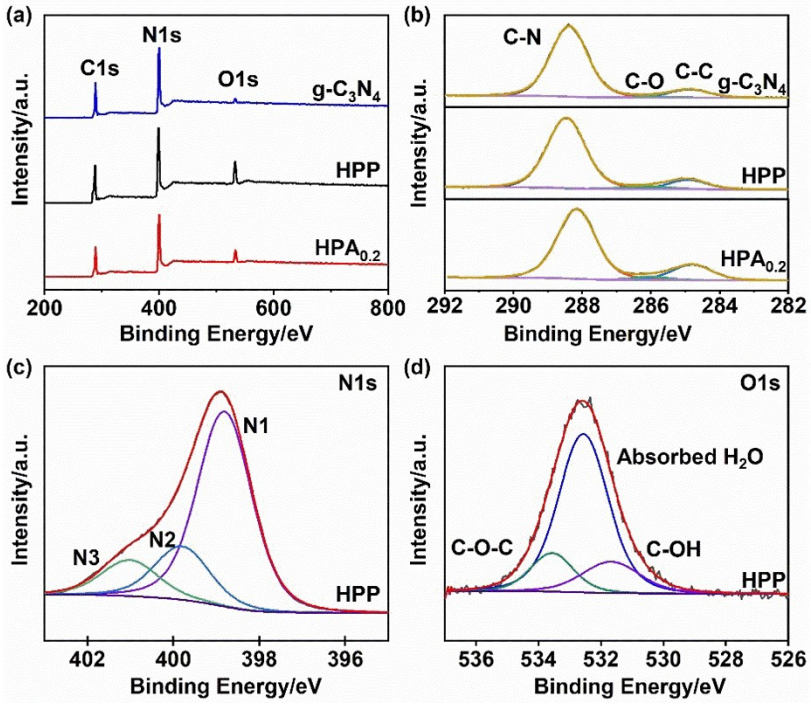

Figure S8. a) XPS spectra, b) C 1s XPS of of g-C_3N_4, HPP and $HPA_{0.2}$. c) N 1s, and d) O 1s of HPP.

Table S1. The relative N species concentration (%) of g-C_3N_4 and $HPA_{0.2}$ from XPS spectra of N1s.

Sample	N1/%	N2/%	N3/%	N1/N2
g-C_3N_4	63.26	20.88	15.86	3.03
$HPA_{0.2}$	62.29	23.77	13.94	2.62

.

Table S2. The relative element percentages (at%) of g-C_3N_4 and $HPA_{0.2}$ from XPS.

Sample	C (at %)	N (at %)	O (at %)	C/N
g-C_3N_4	36.86	60.42	2.72	0.61
$HPA_{0.2}$	36.78	56.20	7.02	0.65

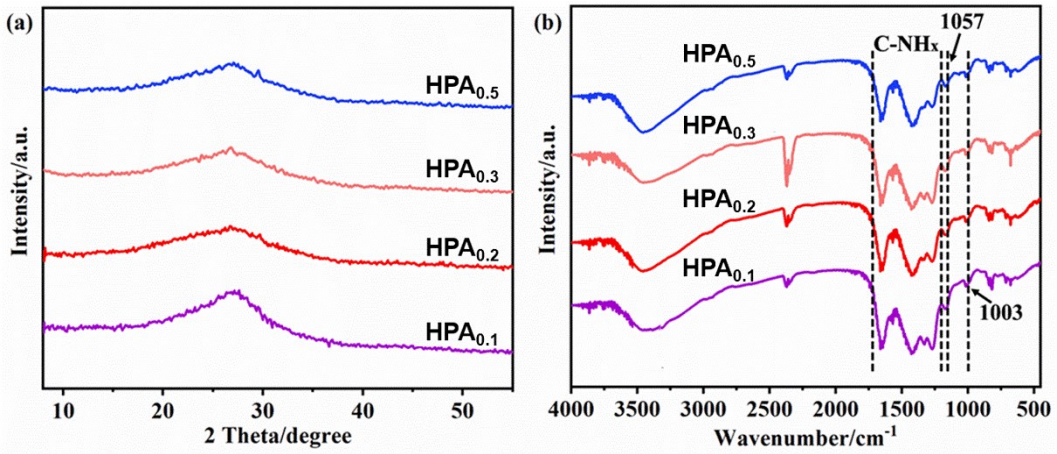

Figure S9. a) XRD patterns, b) FTIR spectra of $HPA_{0.1}$, $HPA_{0.2}$, $HPA_{0.3}$, and $HPA_{0.5}$.

The intensity of XRD peaks (Figure S9a) of HPA become wider and slightly left shift with increasing formic acid usage, indicating the destruction of interlayer periodic structure due to the presence of oxygen species between layers.[4] Compared with g-C_3N_4, it was worth noting that two new sharp peaks at 1003 and 1157 cm^{-1} appeared in the FTIR spectrum (Figure S9b)

of all HPA samples, which were ascribed to the vibration of C-O-C.[5,6] Furthermore, the additional absorption of all the HPA samples between 3400 and 3600 cm^{-1} was assigned to -OH, and the C-NH_x peaks at 1200 and 1700 cm^{-1} were progressively weaker with increasing the amount of formic acid, altogether demonstrating the loss of -NH_x and the introduction of C-O species.

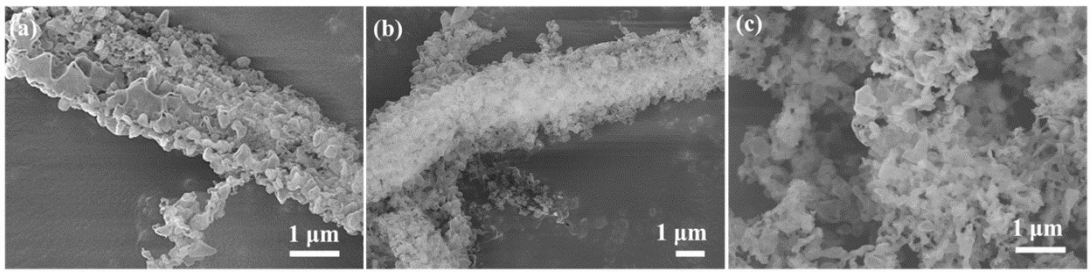

Figure S10. SEM images of (a) $HPA_{0.1}$, (b) $HPA_{0.3}$, (c) $HPA_{0.5}$.

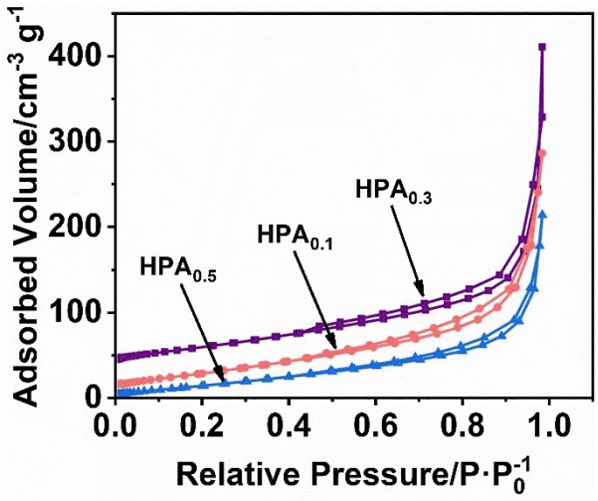

Figure S11. N_2 adsorption isotherms of $HPA_{0.1}$, $HPA_{0.3}$, and $HPA_{0.5}$.

Table S3. Photocatalytic H_2 production performance comparison of various nanostructured g-C_3N_4, and the other conjugated polymer photocatalysts.

Catalysts	Reaction conditions	H_2 evolution rate (μmol h^{-1})	H_2 evolution rate (μmol h^{-1} g^{-1})	External quantum yield (EQY)	Internal quantum yield (IQY)	Ref
$HPA_{0.2}$	3 wt% Pt, 100 mL solution (10 vol% methanol), λ > 420 nm	103.79 (10 mg)	10379	15.3 % (λ= 400 nm)	29.4 % (λ= 400 nm)	This work
PTCN	1 wt % Pt, 100 mL solution (20 vol% methanol), λ > 420 nm	67 (10 mg)	670	5.68 % (λ= 420 nm)		7
PCNT	3 wt% Pt, 100 mL solution (10 vol% TEOA), λ ⩾ 420 nm	101 (20 mg)	2020	4.32 % (λ= 420 nm)		8
Nanomesh	3 wt% Pt, 100 mL solution (10 vol% TEOA), λ> 420 nm	85.1 (10 mg)	8510	5.1 % (λ= 420 nm)		9
CN aerogels	3 wt% Pt, 100 mL solution (10 vol% TEOA, λ > 420 nm	30 (20 mg)	600	3.1 % (λ=420 nm)		10
OCNA-6	3 wt% Pt, 100 mL solution (10 vol% TEOA), λ> 420 nm	16.57 (40 mg)	662.8	7.43 % (λ=420 nm)		11
CN-6	5 mg Pt, 10 vol% TEOA, λ > 395 nm	75.1 (20 mg)	1502	N/A		12
3D foam	3 wt% Pt, 100 mL solution (10 vol% TEOA), λ > 420 nm	111.9 (100 mg)	1119	2.27 % (λ=450 nm)		13
FCN-5	1.5 wt % Pt, 300 mL solution (10 vol% TEOA), λ > 400 nm	59 (100 mg)	590	3.91 % (λ=420 nm)		14

CNF-4	100 mL real water matrices (TEOA as the sacrificial agent), λ > 420 nm	32.9 (20 mg)	657.9	N/A		15
PCNM	3 wt% Pt, 25 mL water, 3 mL TEOA, λ > 420 nm	29 (10 mg)	2900	N/A		16
PI/Ag-1	40 ml mixed solution of water/methanol (3:1 by volume), λ ⩾ 420 nm	6.64 (25 mg)	166.1	N/A		17

Table S4. The relative element percentages (at%) of $HPA_{0.1}$, $HPA_{0.2}$, $HPA_{0.3}$, and $HPA_{0.5}$ from XPS.

Sample	C	N	O	C/N
$HPA_{0.1}$	38.70	57.37	3.93	0.67
$HPA_{0.2}$	36.78	56.20	7.02	0.65
$HPA_{0.3}$	37.99	54.87	7.14	0.69
$HPA_{0.5}$	40.07	50.14	9.79	0.80

As shown in Table S4, with the amount of formic acid increases from $HPA_{0.1}$, $HPA_{0.2}$, $HPA_{0.3}$, to $HPA_{0.5}$, the O content (at%) was gradually increased but the N content (at%) was decreased.

Table S5. The relative percentages (at%) of the nitrogen species for $HPA_{0.1}$, $HPA_{0.2}$, $HPA_{0.3}$, and$HPA_{0.5}$ obtained from XPS.

Sample	N1/%	N2/%	N3/%
$HPA_{0.1}$	64.85	20.46	14.69
$HPA_{0.2}$	62.29	23.77	13.94
$HPA_{0.3}$	64.32	22.78	12.90
$HPA_{0.5}$	66.37	22.43	11.20

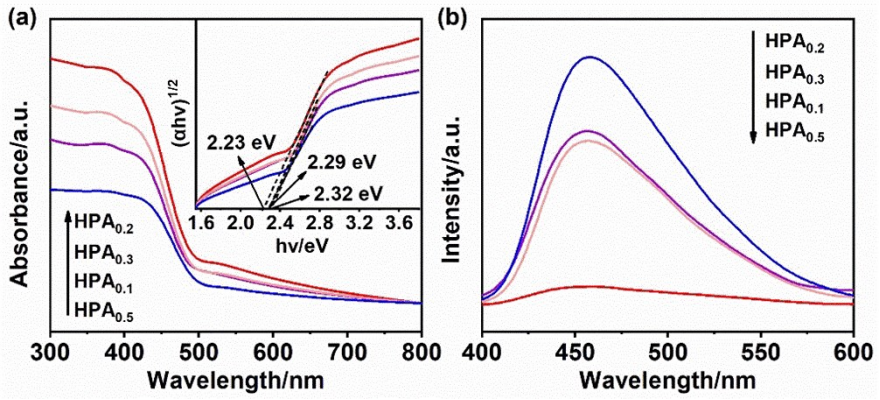

Figure S12. a) UV/Vis spectra and bandgap energies, b) PL spectra of $HPA_{0.1}$, $HPA_{0.2}$, $HPA_{0.3}$, and $HPA_{0.5}$.

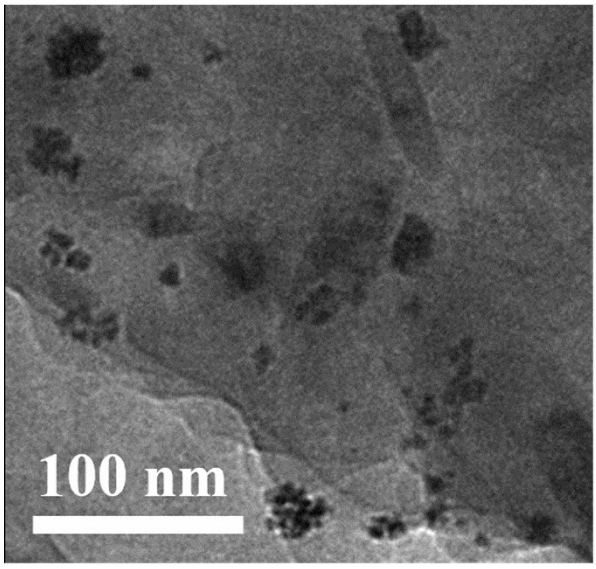

Figure S13. TEM image of Pt/ g-C_3N_4 after photocatalytic reaction.

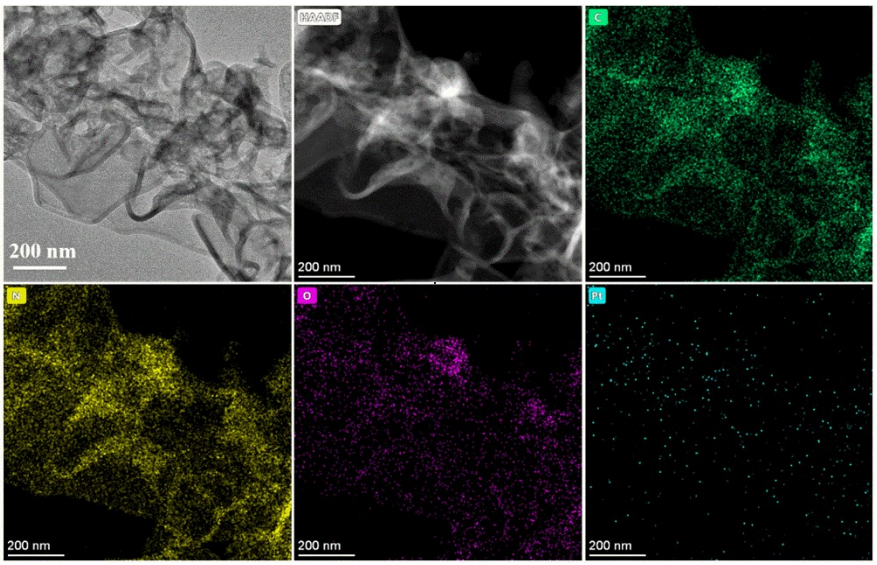

Figure S14. HAADF-STEM image and the corresponding HAADFSTEM-EDS C, N, O element mapping images of Pt/$HPA_{0.2}$ after photocatalytic reaction.

Table S6. The relative element percentages (at%) of $HPA_{0.2}$ before and after long-time run from the Energy-dispersive X-ray spectrum (EDS).

Samples	C	N	O
$HPA_{0.2}$ (before)	34.55	53.35	12.10
$HPA_{0.2}$ (after)	34.80	53.29	11.91

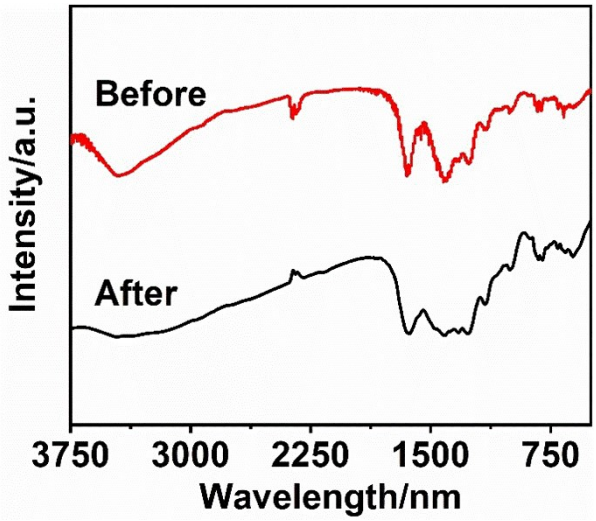

Figure S15. FTIR spectra of $HPA_{0.2}$ before and after the photocatalytic react.

References

1 L. Chen, Y. Wang, C. Wu, G. Yu, Y. Yin, C. Su, J. Xie, Q. Han and L. Qu, *Nanoscale*, 2020, **12**, 13484-13490.
2 M. Qureshi, K. Takanabe, *Chem. Mater.*, 2017, **29**, 158-167.
3 C. Wu, G. Yu, Y. Yin, Y. Wang, L. Chen, Q. Han, J. Tang and B. Wang, *Small*, 2020, **16**, 2003162.
4 Y. Wang, M. K. Bayazit, S. J. A. Moniz, Q. Ruan, C. C. Lau, N. Martsinovich and J. Tang, *Energy Environ. Sci.*, 2017, **10**, 1643-1651.
5 Z. Lu, G. Chen, S. Siahrostami, Z. Chen, K. Liu, J. Xie, L. Liao, T. Wu, D. Lin, Y. Liu, T. F. Jaramillo, J. K. Nørskov and Y. Cui, *Nat. Catal.*, 2018, **1**, 156-162.
6 H. Yu, L. Shang, T. Bian, R. Shi, G. I. Waterhouse, Y. Zhao, C. Zhou, L. Z. Wu, C. H. Tung and T. Zhang, *Adv. Mater.*, 2016, **28**, 5080-5086.
7 S. Guo, Z. Deng, M. Li, B. Jiang, C. Tian, Q. Pan and H. Fu, *Angew. Chem. Int. Ed.*, 2016, **55**, 1830-1834.
8 M. Wu, J. Zhang, B. B. He, H. W. Wang, R. Wang and Y. S. Gong, *Appl. Catal., B*, 2019, **241**, 159-166.

9 Q. Han, B. Wang, J. Gao, Z. Cheng, Y. Zhao, Z. Zhang and L. Qu, *ACS Nano*, 2016, **10**, 2745-2751.
10 H. Ou, P. Yang, L. Lin, M. Anpo and X. Wang, *Angew. Chem. Int. Ed.*, 2017, **56**, 10905-10910.
11 W. Jiang, Q. Ruan, J. Xie, X. Chen, Y. Zhu and J. Tang, *Appl. Catal., B*, 2018, **236**, 428-435.
12 K. Kailasam, J. D. Epping, A. Thomas, S. Losse and H. Junge, *Energy Environ. Sci.*, 2011, **4**, 4668.
13 Q. Guo, Y. Zhang, H. S. Zhang, Y. Liu, Y. J. Zhao, J. Qiu and G. Dong, *Adv. Funct. Mater.*, 2017, **27**, 1703711.
14 Y. Li, Z. Ruan, Y. He, J. Li, K. Li, Y. Jiang, X. Xu, Y. Yuan and K. Lin, *Appl. Catal., B*, 2018, **236**, 64-75.
15 H. Wang, Y. Wu, M. Feng, W. Tu, T. Xiao, T. Xiong, H. Ang, X. Yuan and J. W. Chew, *Water Res.*, 2018, **144**, 215-225.
16 Q. Liang, Z. Li, X. Yu, Z. H. Huang, F. Kang and Q. H. Yang, *Adv. Mater.*, 2015, **27**, 4634-4639.
17 X. Zhao, X. Yi, X. Wang, W. Chu, S. Guo, J. Zhang, B. Liu and X. Liu, *Appl. Surf. Sci.*, 2020, **502**, 144187.